9th Asia-Pacific Conference on Plasma Physics, 21-26 Sep, 2025 at Fukuoka

The radial evolution of parametric decay instability incorporating temperature anisotropy in the near-sun solar wind

Hayato Saguchi[1], Yohei Kawazura[2, 1], Munehito Shoda[3], Yuto Katoh[1]
[1] Department of Geophysics, Graduate School of Science, Tohoku University, [2] School of Data Science and Management, Utsunomiya University, [3] Department of Earth and Planetary Science, The University of Tokyo
e-mail (speaker): saguchi.hayato.s4@dc.tohoku.ac.jp

Alfvén waves (AWs) are thought to play a crucial role in coronal heating and the solar wind acceleration. Indeed, magnetohydrodynamic (MHD) simulations that incorporate AW turbulence driven by the parametric decay instability (PDI) successfully reproduce both phenomena [1, 2]. It has also been demonstrated that PD is enhanced by temperature anisotropy [3]. It is necessary to investigate the relation between temperature anisotropy and PDI further.

To examine the effect of temperature anisotropy on the radial evolution of PDI, we use two dispersion relations of PDI. One is derived from isotropic MHD equations [4, 5] and the other is derived from CGL equations, which are anisotropic MHD equations with double-adiabatic closure [3].

Using two dispersion relations, we compute the maximum linear growth rate divided by the mother wave angular frequency γ_{max}/ω_0 between $R \cong 100{,}000km$ and $R \cong 30R_\odot$ on the five kinds of expanding scenarios: (1) Simple Adiabatic—simple spherical expansion $B \propto R^{-2}$ and $\rho \propto R^{-2}$ with adiabatic closures; (2) PSP-Consistent Adiabatic—scalings $B \propto R^{-1.66}$ and $\rho \propto R^{-2.59}$ based on Parker Solar Probe (PSP) [6] with the same adiabatic closures; (3) Isothermal Parallel and Perpendicular Adiabatic —PSP scalings for B and ρ with isothermal parallel temperature $T_\parallel$ and adiabatic $T_\perp$; (4) Temperature profile based on [7] with simple spherical B and ρ scalings —realistic 3-D MHD temperature profiles with simple spherical expansion $B \propto R^{-2}$ and $\rho \propto R^{-2}$; and (5) Temperature profile based on [7] with PSP scalings for $B \propto R^{-1.66}$ and $\rho \propto R^{-2.59}$. We simultaneously plot the existence condition of the mother wave [3]:

$f(R) = 1 + \frac{\beta_\parallel(\frac{T_\perp}{T_\parallel}-1)}{2(1+B_\perp^2)}$. When $f(R) \leq 0$, the mother wave cannot be sustained and PDI does not occur. Note that we do not consider the expansion effect and the radial dependence of mother wave frequency that was considered in several studies[1, 2, 8].

The result of (1) shows the difference between the isotropic result and the anisotropic result. In the isotropic one, maximum linear growth rate tends to increase with heliocentric distance, which is consistent with [8], while in the anisotropic one maximum linear growth rate tends to decrease with heliocentric distance [Figure 1]. This suggests that PDI does not occur in the distant solar wind satisfying the adiabatic condition. The result of (2) shows that both the isotropic-MHD and anisotropic-CGL results exhibit a monotonic increase in growth rate with heliocentric distance. This behavior arises because, under the adopted scalings, β continuously declines while the temperature anisotropy $T_\perp/T_\parallel$ continuously grows. The result of (3) shows that when β is low, both the isotropic-MHD and anisotropic-CGL results again exhibit a monotonic increase in growth rate. However, at high β the anisotropic-CGL growth rate decreases, whereas the isotropic-MHD rate continues to increase. The result of (4) and (5) shows that because the imposed temperature anisotropy remains finite from 10 solar radii, the anisotropic growth rate never vanishes but instead plateaus at an approximately constant value.

In conclusion, our results demonstrate that radial expansion modifies the temperature anisotropy and, in turn, suppresses PDI growth, suggesting that the temperature anisotropy should be included in PDI-driven Alfvén wave turbulence model.

References
[1] Shoda et al., 2018, DOI: 10.3847/1538-4357/aac218
[2] Shoda et al., 2019, DOI: 10.3847/2041-8213/ab2b45
[3] Tenerani et al., 2017, DOI:10.3847/1538-4357/aa9bef
[4] Derby 1978, DOI: 10.1086/156451
[5] Goldstein 1978, DOI: 10.1086/155829
[6] Huang et al., 2020, DOI: 10.3847/1538-4365/ab74e0
[7] Meng et al., 2015, DOI: 10.1093/mnras/stv2249
[8] Réville et al., 2018, DOI: 10.3847/1538-4357/aadb8f

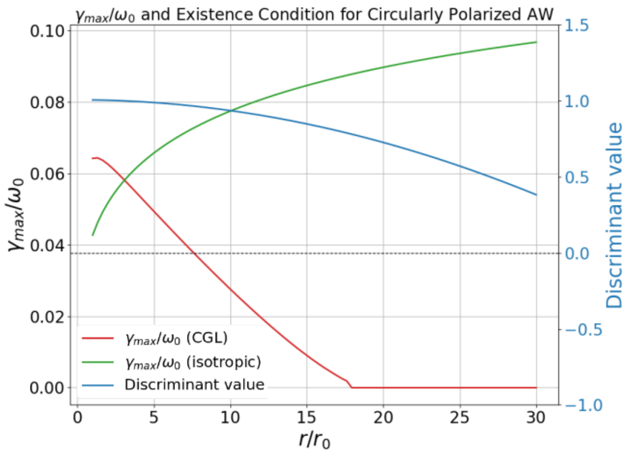

Figure 1. The radial evolution of the maximum linear growth rate between $R \cong 100{,}000km$ and $R \cong 30R_\odot$ on the expanding scenario (1).

Note: Abstract should be in (full) double-columned one page